X-RAY EMISSION OF A SAMPLE OF LINER GALAXIES

O. González-Martín*, J. Masegosa & I. Márquez

Instituto de Astrofísica de Andalucía (CSIC), Apdo 3004, 18080 Granada, Spain

ABSTRACT

We report the results from an homogeneous analysis of the X-ray (ACIS-S/Chandra) data available for a sample of 52 LINER galaxies. The X-ray morphology has been classified attending to their nuclear compactness in the hard band (4.5–8.0 keV), into 2 categories: AGN-like nuclei (with a clearly identified unresolved nuclear source) and Starburst-like nuclei (without a clear nuclear source). 60% of the total sample are classified as AGNs, with a median luminosity of $\mathrm{L_X(2.0-10.0\,keV) = 2.5 \times 10^{40}\,erg\,s^{-1}}$, which is an order of magnitud higher than that for SB-like nuclei. All X-ray morphology, spectral fitting and Color-Color diagrams allow to conclude that a high percentage of LINER galaxies host AGN nuclei.

Key words: galaxies, AGN, LINER, X-ray, Chandra.

1. INTRODUCTION

LINERs are very common in the nearby universe. Pioneering works already estimate that at least 1/3 of all the spiral galaxies are LINERs (Heckman et al. 1980). More than two decades after they were clasified, there is still an ongoing strong debate on the origin of the energy source in LINERs, with two main alternatives for the ionizing source being explored: either a low luminosity AGN (Filippenko & Halpern, 1984), or a thermal origin from massive star formation (Filippenko & Terlevich, 1992) and/or from shock heating mechanisms resulting from the massive stars evolution (Fosbury et al. 1978 and Dopita 1976). The search for a compact X-Ray nucleus in LINERs is indeed one of the most convincing evidences about their AGN nature. The excellent resolution of Chandra allows an investigation of the X-Ray nuclear properties of these galaxies.

*e-mail address: omaira@iaa.es

2. SAMPLE & DATA PROCESS

All the 476 LINER galaxies in the compilation by Carrillo et al. (1999) have been searched by coordinates in Chandra archives. The final sample comprises 52 galaxies with high S/N ratio and optically reidentified.

The data products were analyzed in an uniform, self-consistent, manner using *CXC Chandra Interactive Analysis of Observations* (CIAO) software version 3.1. The spectral analysis was done with *XSPEC* (version 11.3.2). Level 2 event data from ACIS instrument have been extracted from Chandra archive. Time intervals with high background levels have been excluded.

3. SPECTRAL FITTING & LUMINOSITIES

For the source selection, we made use of the nuclear positions from NVSS and 2MASS data base. Nuclear spectra were extracted using regions defined to include as many photons coming from the source as possible, but at the same time minimizing contamination from nearby sources and background. The background region was defined as either a source-free circular annulus or several circles surrounding each source, to take into account the spatial variations of the diffuse emission and to minimize effects related to the spatial variation of the CCD response. In order to use the χ^2 statistic, the data were grouped to include at least 20 counts per spectral bin, before background substraction. For the spectral fitting any events with energies above 10.0 keV or below 0.5 keV have been excluded. The spectra in the 0.5-10.0 keV passband were modelled with a single [MEKAL (ME), Raymond-Smith (RS) or Power Law (PL)] component first and second with a two component [ME+PL or RS+PL] model. Single models are representative for sources dominated either by thermal emission, or non-thermal emission, and two component models correspond to composite objects. Note that number counts were sufficient to employ detailed spectral fitting in 24 out of 52 objects.

The luminosities and fluxes of the individual nuclear

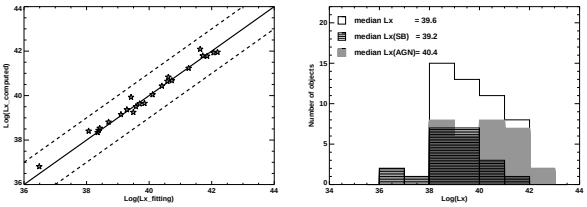

Figure 1. (left): Luminosity estimation versus real luminosity. (right): Luminosity histogram for the whole sample and clasified objects.

sources have been computed based on the best-fit model for the 24 galaxies above. We have done an empirical calibration from these 24 objects with high signal-to-noise ratio from flux estimation, assuming an intrinsic power law slope of 1.8, corrected for Galactic absortion. In Fig. 1 (left) our estimated luminosity is plotted versus the value obtained from the direct integration of the spectral energy distribution. The 2.0–10.0 keV luminosities are therefore provided for the whole sample, using the spectral energy distribution fit, when it is available, and from this calibration otherwise.

4. MORPHOLOGICAL CLASSIFICATION

We have classified the nuclear morphology attending to the compactness in the hard band (4.5 to 8.0 keV):

- **AGN-like nuclei:** Clearly identified unresolved nuclear source in the hard band. 59.6% (31/52) has been clasified as AGN-like nuclei in our sample and their median luminosity is $\mathrm{L_X(2-10\ keV) = 2.5 \times 10^{40} erg\ s^{-1}}$.
- **Starburst-like nuclei (SBs):** Objects without a clear nuclear source in the hard band. 40.4% of the sample of LINERs fall in this classification and their median luminosity is $\mathrm{L_X(2-10\ keV) = 1.0 \times 10^{39}\ erg\ s^{-1}}$.

5. COLOR-COLOR DIAGRAMS

The colors of the nuclear sources have been defined as the ratio of counts observed in the following energy bands: 0.6 to 0.9, 0.9 to 1.2, 1.2 to 1.6, 1.6 to 2.0, 2.0 to 4.5, and 4.5 to 8.0 keV. The bands were chosen in order to maximize the detection as well as to obtain a good characterization of the spectra. In the last energy band, the range from 6.0 to 7.0 keV has been excluded to avoid the possible contamination due to the FeK emission line. Therefore, 3 colors has been defined ($\mathrm{Q_A}$, $\mathrm{Q_B}$ and $\mathrm{Q_C}$) as Q=(Hard-Soft)/(Hard+Soft). Sinthetic colors were computed for PL, RS and PL+RS models (see Fig.2). We have only considered the data with error less than 30%. In the $\mathrm{Q_B}$ versus $\mathrm{Q_C}$ plot (Fig. 2, bottom) we can see that

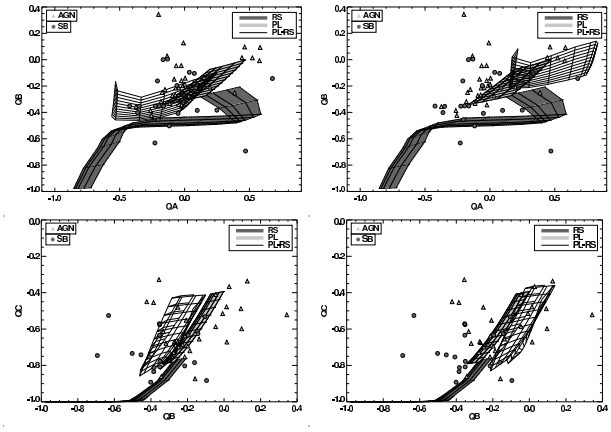

Figure 2. Color-color diagrams for a RS model , PL model and combinated model for $\mathrm{N_H = 10^{20}\ cm^{-2}}$ (left) and $\mathrm{N_H = 10^{22}\ cm^{-2}}$ (right). QB versus QA (top) and QC versus QB (bottom).

$\mathrm{Q_C}$ is a good AGN activity estimator. Objects classified as AGN-like nulcei have high values of $\mathrm{Q_C}$. However, not only a few objects classified as SB-like have a high $\mathrm{Q_C}$, but also most of the objects classified as SB are not in the thermal model grid. Therefore, the use of Color-Color diagrams allows to also analyze the properties of the nuclear sources for which the spectral fitting is not possible.

6. CONCLUSIONS

Morphologically, 60% of LINERs have been classified as AGN-like candidates, with median luminosity 10 times higher than that of SB-like objects (Fig. 1, right). Color-Color diagrams are a valid tool to estimate physical parameters, specially interesting to be used when the spectral fit is not possible. Both thermal and non-thermal contributions are required for the spectral fitting of most of the objects. Color-Color diagrams have confirmed this result. An empirical calibration for estimating X-ray luminosities ($\mathrm{L_X(2.0-10.0\ keV)}$) has been done based on total counts, which allows a reliable estimation when the spectral fitting is not possible.

REFERENCES

Carrillo R. et al., 1999, Rev. Mex. A&A, 35, 18.

Dopita M.A., 1976 ApJ, 209, 395.

Filippenko A. V. & Halpern, J. P. 1984 ApJ, 285, 458.

Filippenko, A. V., & Terlevich, R. 1992 ApJ, 397, L79.

Fosbury R. A. E. et al. 1978 MNRAS, 183, 549.

Heckman T.M. et al., 1980, A&AS, 40, 295.

Ho L. C. et al., 1985, ApJ, 549, L51.